Eur. Phys. J. Spec. Top. (2022) 231:833–845
https://doi.org/10.1140/epjs/s11734-021-00314-7

THE EUROPEAN PHYSICAL JOURNAL SPECIAL TOPICS

Review

Biochaos in cardiac rhythms

Augusto Cheffer[1,a] and Marcelo A. Savi[1,b]

[1] Center for Nonlinear Mechanics, COPPE - Department of Mechanical Engineering, Universidade Federal do Rio de Janeiro, P.O. Box 68.503, Rio de Janeiro, RJ, Brazil

Received 8 April 2021 / Accepted 25 October 2021 / Published online 9 November 2021

Abstract Biological rhythm is an essential characteristic of natural systems that can present regular or irregular dynamics, which can be associated with normal or pathological functioning. In this regard, nonlinear dynamics perspective is able to connect biorhythm with functioning characteristics. This paper investigates the heart dynamics by considering a mathematical model that is built from three coupled nonlinear oscillators. The main strategy is to investigate natural pacemaker behavior, establishing its influence on the electrical activity of the heart represented by electrocardiograms (ECGs). Different kinds of pacemaker behaviors are treated, dedicating special attention to chaotic rhythms.

1 Introduction

Biological rhythm is an essential characteristic of natural systems where complexity and diversity are due to intrinsic nonlinearities [1]. Rhythms can present regular or irregular dynamical behaviors, which can be associated with normal or pathological functioning. In this regard, dynamical analysis is able to connect biorhythm (periodic, quasi-periodic or chaotic) with functioning characteristics (normal or pathological), being useful to identify pathologies. Some examples of biosystems where the rhythms can be employed to characterize their functioning behaviors include heart, brain, cells and molecules.

Several studies suggest that chaotic dynamics is desirable for biological systems to increase their adaptability [2–4]. According to Pool [2], "chaos may provide a healthy flexibility to the heart, brain, and other parts of the body". Classical dynamical invariants are widely employed to characterize biochaos, including power spectrum, fractal dimension and short term predictability, but the most widespread method is the Lyapunov exponents. Chaos identification in cardiac and neural systems, which can be performed by time series analysis, has been treated in several research efforts [5–9].

Heart is the essential organ of the cardiac system being responsible for its most important dynamical characteristics. The mammalian heart is a hollow muscular organ with four cavities (two atria and two ventricles), being responsible for pumping blood through all tissues and organs of the body. Its functioning is driven by an electrical network composed by sinoatrial node (SA), atrioventricular node (AV) and His–Purkinje complex (HP) [10,11]. SA node is the natural pacemaker where the initial stimulus occurs, being conducted by atria, contracting them. Upon reaching AV node, secondary pacemaker, the stimulus excites the bundle of His and the Purkinje fibers in sequence, producing ventricles contraction [12].

The electrocardiogram (ECG) is the most widespread method to measure cardiac activity. ECG records the activity of the heart as waveforms through electrical impulses generated during cardiac functioning. Typically, the ECG pattern presents P wave, QRS complex and T wave. P wave represents the impulse generated by the SA node; QRS complex is formed by ventricular contraction; and T wave reflects ventricular repolarization when cardiac cells return to a state in which they are ready to react to another stimulus. Although normal ECG is apparently periodic, it presents a variability called heart rate variability (HRV), which can be measured from R–R intervals evaluated from the distance between two subsequent R waves [13]. Due to unavoidable noise occurrence, it is necessary to use some signal processing techniques [14], such as detection of R peaks [15,16] and calculation of HRV and breathing [13,17]. A comparison between deterministic chaos and random noise for the heart rhythm is found in [18].

Glass [11] presented a historical review about chaos in heart rhythms concluding that normal heart rate variability is not related to chaotic dynamics. Studies with opposite statements are based on operational definitions that do not properly capture the chaotic properties. On the other hand, there are evidences of chaos in heart pathological behaviors discussed in several references from time series analysis [19,20]. Herbschleb et al. [5] performed a frequency analysis in canine EGCs with

[a] e-mail: augusto.cheffer@poli.ufrj.br
[b] e-mail: savi@mecanica.coppe.ufrj.br (corresponding author)

ventricular fibrillation (VF). Bayly et al. [21] employed ECGs recorded from pig hearts to explore experimental procedures and organization measurements, quantifying spatio-temporal behavior during VF. Chen et al. [6] analyzed VF mechanisms using computational mapping techniques. Skanes et al. [7] highlighted the presence of spatio-temporal organization during atrial fibrillation (AF) in sheep hearts. Zhang et al. [22] showed that stochastic release of acetylcholine regulator in the vicinity of the SA node leads to responses that exhibit chaotic characteristics.

Some research efforts indicated that a chaotic response can be predicted from short time series [23–25], being of special interest for cardiac dynamics analysis. Determinism and predictability in heart time series is explored by [26,27]. Govindan et al. [28] investigated the existence of deterministic chaos in human ECGs using surrogate data analysis, short term prediction, correlation dimension and Lyapunov exponents. Regression methods for predictions related to short time series are treated by [29–31].

Multiscale characteristic of heartbeat time series is investigated by Peng et al. [33], being extended by Alvarez-Ramirez et al. [34] with the introduction of time lags into detrended fluctuation analysis. Time delays were identified in various cardiac feedback control loops. Multiscale methods have been employed to analyze different time scale organization and non-equilibrium dynamics, presenting better results in situations where the classical measures as power spectra and Lyapunov exponents do not present proper results. A review of these methods is presented by Costa et al. [35].

Besides time series analysis, heart dynamics can be analyzed by mathematical model perspective. The first mathematical model to describe heart dynamics was proposed by van der Pol and van der Mark [36] establishing an analogy between heartbeats and electrical circuits described by nonlinear oscillators. Some studies treated different aspects of AF, such as modeling of atrial tissue under AF [37] and the description of mechanisms that sustain AF [38]. Different approaches are also presented for VF including reentry mechanisms that cause arrhythmias [39]; restitution properties and spiral wave behaviors of cardiac action potential [40,41]. A review of the most relevant studies about mechanisms of initiation and maintenance of VF is found in [42]. Nash and Panfilov [43] developed a model of an excitable tissue able to reproduce both flutter and fibrillation.

Grudzinski and Zebrowski [44] proposed a more accurate natural pacemaker mathematical model by a modification of the original van der Pol (vdP) oscillator. To describe cardiac system, several studies developed models by coupling modified vdP oscillators. Dos Santos et al. [45] used two asymmetrically coupled oscillators to represent heart dynamics. Gois and Savi [10] proposed bidirectional and time delayed coupling of three oscillators that represent SA and AV nodes and HP complex functioning. Cheffer et al. [46] improved the three-coupled oscillator model due to [10] by modifying coupling terms. A qualitative comparison between experimental and model-generated ECG signals showed that the model is able to reproduce several biorhythms. Nonlinear tools were also applied to help rhythm characterization and bifurcation analysis, showing possible routes from normal to pathological responses.

Based on FitzHugh-Nagumo (FHN) type equations, Ryzhii and Ryzhii [47,48] proposed a network of strongly coupled oscillators with time delay to model cardiac pacemakers. FHN equations were also employed to improve branch blocks modeling. Cardadilli et al. [49] proposed a model by coupling four modified vdP oscillators, representing SA and AV nodes and right and left bundle branches.

An attractive approach for clinical purposes is the application of control methods in cardiac rhythms. Garfinkel et al. [50,51] performed the pioneer experiment of chaos control on biomechanical systems, using OGY method [52] on rabbit cardiac muscle. Ferreira et al. designed a controller for a natural pacemaker [44] using a time-delayed feedback control method [53]. By applying the same technique, Ferreira et al. [54] performed chaos control for ECG signals generated by the cardiac system model proposed by [10]. Lounis et al. [55] used high-order chaos control applied to cardiac model due to Quiroz-Juarez et al. [56]. An active control technique based on Lyapunov stabilization is presented by Khan and Nigar [57] combining synchronization in fractional-order chaotic system with disturbance and uncertainty.

Random aspects are investigated by considering different perspectives. An interesting perspective points that nonlinearities and randomness work together to promote natural rhythms. By analyzing canine ECGs with fibrillation, Kaplan and Cohen [15] concluded that fibrillation is similar to a random signal, showing that random-like (nonchaotic) response can be generated by a deterministic system. Yates and Benton [58] discussed challenges of choosing which type of analysis (deterministic or statistical) is more interesting to deal with human cardiovascular data. Cheffer and Savi [59] showed that pathological rhythms can be generated by nondeterministic aspects represented by random couplings. Cheffer et al. [60] developed a probabilistic approach based on Random Matrix Theory to investigate coupling uncertainties.

This paper deals with biochaos in cardiac systems considering that the electrical activity of the heart is modeled by three coupled nonlinear oscillators that represent SA node, AV node and HP complex [10]. Based on that, synthetic ECG can be represented describing the cardiac system behavior. The strategy is to investigate the influence of different kinds of behaviors of the natural pacemaker, the sinoatrial node, on the ECG responses. A global comprehension of the natural pacemaker behavior is provided by the analysis of bifurcation diagrams that are built varying dissipation and external stimulus of the SA oscillator. This analysis allows one to identify different kinds of behaviors including chaotic responses. The influence of these kinds of behaviors on the electrical activity of the heart,

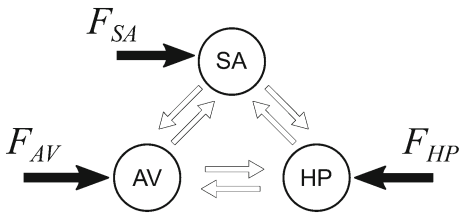

Fig. 1 Conceptual model of the general cardiac functioning

represented by ECGs, is investigated establishing a connection with distinct pathologies. Special attention is dedicated to the effect of chaotic driven signals.

2 Mathematical model

Electrical activity of the heart is often modeled by the van der Pol oscillator since its dynamic response presents typical characteristics of biological systems such as limit cycle, synchronization and chaos [10,44]. Besides that, van der Pol equation has oscillation amplitude that does not depend on the oscillation rate. The model proposed by Grudzinski and Zebrowski [44] is a modification of the original van der Pol oscillator including a restitution force described by a cubic function being expressed as follows:

$$\ddot{x} + \alpha\,\dot{x}(x-\nu_1)(x-\nu_2) + \frac{x(x+d)(x+e)}{d\,e} = F(t), \tag{1}$$

where α defines the pulse shape, characterizing the time when the heart receives the stimulus; ν_1 and ν_2 determine the signal amplitude, and to preserve the self-excitatory nature, $\nu_1\nu_2 < 0$; d and e are system parameters; and $F(t)$ is an external stimulus.

The stability analysis of equilibrium points through the eigenvalues of the Jacobian matrix shows that the system exhibits 3 equilibrium points $\{x, \dot{x}\}$: $\{0,0\}$, $\{-d,0\}$ and $\{-e,0\}$, being respectively characterized by center, saddle and sink.

The cardiac system is modeled from the coupling of three nonlinear oscillators representing SA node, AV node and HP complex (HP) [10], as the conceptual model presented in Fig. 1. Asymmetrical and bidirectional connections are employed to build a general model that is capable to reproduce the electrical activity of the heart including normal and pathological functioning. The coupling connections uses time-delayed terms to represent the transmitting time spent among each one of the oscillators. Under these assumptions, central nervous system stimuli are represented by self-excitatory behavior which means that external stimulus refers to situations different of the normal functioning. On this basis, the cardiac system is governed by the following equations [46]:

$$\begin{aligned}
\dot{x_1} &= x_2\\
\dot{x_2} &= F_{SA}(t) - \alpha_{SA}\,x_2(x_1-\nu_{SA_1})(x_1-\nu_{SA_2})\\
&\quad - \frac{x_1(x_1+d_{SA})(x_1+e_{SA})}{d_{SA}\,e_{SA}}\\
&\quad - k_{AV-SA}\,x_1 + k^{\tau}_{AV-SA}\,x_3^{\tau_{AV-SA}}\\
&\quad - k_{HP-SA}\,x_1 + k^{\tau}_{HP-SA}\,x_5^{\tau_{HP-SA}}\\
\dot{x_3} &= x_4\\
\dot{x_4} &= F_{AV}(t) - \alpha_{AV}\,x_4(x_3-\nu_{AV_1})(x_3-\nu_{AV_2})\\
&\quad - \frac{x_3(x_3+d_{AV})(x_3+e_{AV})}{d_{AV}\,e_{AV}}\\
&\quad - k_{SA-AV}\,x_3 + k^{\tau}_{SA-AV}\,x_1^{\tau_{SA-AV}}\\
&\quad - k_{HP-AV}\,x_3 + k^{\tau}_{HP-AV}\,x_5^{\tau_{HP-AV}}\\
\dot{x_5} &= x_6\\
\dot{x_6} &= F_{HP}(t) - \alpha_{HP}\,x_6(x_5-\nu_{HP_1})(x_5-\nu_{HP_2})\\
&\quad - \frac{x_5(x_5+d_{HP})(x_5+e_{HP})}{d_{HP}\,e_{HP}}\\
&\quad - k_{SA-HP}\,x_5 + k^{\tau}_{SA-HP}\,x_1^{\tau_{SA-HP}}\\
&\quad - k_{AV-HP}\,x_5 + k^{\tau}_{AV-HP}\,x_3^{\tau_{AV-HP}}
\end{aligned} \tag{2}$$

By considering indexes m and n that can represent SA, AV or HP, and $m \neq n$, equation terms are now explained; k_{m-n} and k^{τ}_{m-n} are coupling coefficients between m and n nodes; and $x_i^{\tau_{m-n}} = x_i(t-\tau_{m-n})$ are delayed terms where τ_{m-n} is the time delay. Although oscillator descriptions do not present spatial aspects, it can capture macroscopic spatial influences. On this basis, $F_m(t) = \rho_m \sin(\omega_m t)$ is an external excitation that has origin in spatiotemporal stimulus and, therefore, it is considered as a reduced-order representation of spatiotemporal aspects. The harmonic form is motivated by AF mechanisms, which are represented by periodic behavior [7,38]. Note that this external stimulus increases the system dimension by introducing an explicit time dependence based on spatiotemporal information.

The ECG is formed by a combination of the signal of each one of the oscillators, being expressed by a linear combination of the state variables given by [10],

$$X = ECG = \beta_0 + \beta_1\,x_1 + \beta_2\,x_3 + \beta_3\,x_5, \tag{3}$$

where β_0, β_1, β_2 and β_3 are parameters. Therefore,

$$\dot{X} = \frac{d}{dt}(ECG) = \beta_1\,x_2 + \beta_2\,x_4 + \beta_3\,x_6. \tag{4}$$

It should be pointed out that the natural pacemaker and the other two oscillators are governed by nonlinear differential equations but since the connection of the three-oscillator model employs time-delayed couplings, the cardiac system is governed by delayed-differential equations (DDEs). This representation is a reduced-order model for the description of the electrical activ-

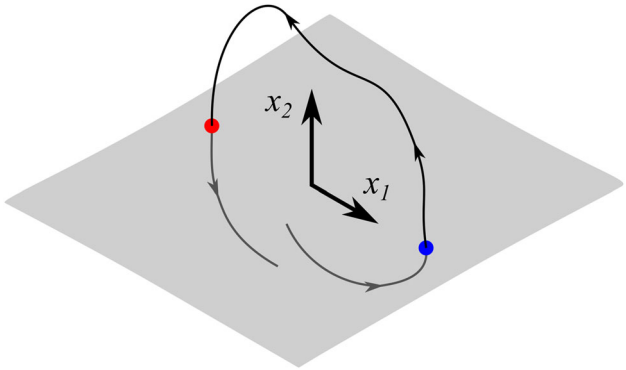

Fig. 2 Poincare map construction employed to build bifurcation diagrams. Poincare section is the set of intersections of system trajectory (black) with secant plane (gray). Red and blue points are related to negative and positive x_2 directions, respectively

ity of the heart since the real problem is a spatiotemporal, multiphysics system. Therefore, its description from coupled oscillators is an interesting simplification that can be useful for different purposes. In this regard, the number of adjustable parameters is justified by the number of phenomena involved.

3 Natural pacemaker

Natural pacemaker behavior is now in focus considering the nonlinear oscillator of the SA node, governed by a nonlinear differential equation. To investigate the possible responses of the natural pacemaker, numerical simulations are carried out employing the fourth-order Runge–Kutta method. A convergence analysis indicates that time steps smaller than 10^{-3} presents error of the order of 10^{-6}, which is considered satisfactory. A global comprehension of the pacemaker behavior is analyzed considering bifurcation diagrams that are built using Poincare maps based on return map associated with a secant section. A section orthogonal to $\{x_1, x_2\}$ in $x_2 = 0$ is adopted and transversal intersections in negative x_2 direction are collected, as schematically shown in Fig. 2. Initial conditions [46] are given by: $\{x_1, x_2\} = \{-0.1, -0.025\}$.

Natural pacemarker behavior is treated by evaluating the influence of two different parameters: dissipation and external stimuli. The analysis is based on bifurcation diagrams where different kinds of behaviors are identified by numbers that are employed from now on as representative of each kind of behavior. The slow quasi-static variation of parameters considers the last state of previous simulation as initial conditions. Besides, the classical algorithm due to Wolf et al. [32] is employed to estimate Lyapunov exponents.

Parameters for natural pacemaker normal functioning are presented in Table 1 that assumes that there is not an external stimulus $F(t) = 0$ [53].

Table 1 Natural pacemaker parameters associated with normal functioning [46]

SA node	
α_{SA}	3
ν_{SA_1}	1
ν_{SA_2}	−1.9
d_{SA}	1.9
e_{SA}	0.55

3.1 Influence of dissipation

The influence of dissipation coefficient α is now of concern. Figure 3 presents the analysis of system response due to parameter variation. A bifurcation diagram is built by considering α in interval $[0.5, 9]$ with steps of 0.1 and simulations with $t \in [0, 1000]$. Different responses identified in the bifurcation diagrams are highlighted by considering phase spaces and time history. Note that bifurcation diagrams indicate regular responses that can be either periodic or quasi-periodic. Lyapunov exponent analysis points that responses are quasi-periodic since an extra null exponent is identified, in addition with time dimension. Besides, it is observed that as α increases, oscillator frequency decreases. It should be pointed out that the typical normal functioning is associated with Response 2 ($\alpha = 3$).

3.2 Influence of external stimulus

This section evaluates the influence of external stimulus by considering a harmonic function, $F(t) = \rho \sin(\omega t)$. On this basis, the investigation is based on two parameters: amplitude (ρ) and frequency (ω). The other parameters (including α) are related to normal functioning of the pacemaker presented in Table 1. In general, external stimulus induces pathological behaviors as atrial and ventricular fibrillation [46].

External stimulus amplitude analysis considers $\rho \in [0, 10]$ with steps of 0.025, simulations with $t \in [0, 5000]$, and a constant frequency is adopted, $\omega = 2.1$ [46]. Figure 4 presents a bifurcation diagram, identifying four responses associated with chaotic-like behaviors. Each response has one positive exponent, which assures the existence of chaos. The following values are obtained for the maximum exponents: Response 4–0.06; Response 5–0.10; Response 6–0.14; Response 7–0.13.

External stimulus frequency is treated by considering $\omega \in [0, 10]$ with steps of 0.025 and simulations with $t \in [0, 5000]$. Amplitude value is constant $\rho = 5.45$ (referring to Response 4 in Fig. 4—first chaotic region) and the other parameters are related to normal functioning of the pacemaker (Table 1). Figure 5 presents bifurcation diagram showing different kinds of behaviors including chaotic-like responses and periodic windows. Selected responses are highlighted showing chaotic-like responses with positive Lyapunov exponents, with the following maximum values: Response 8–0.08; Response

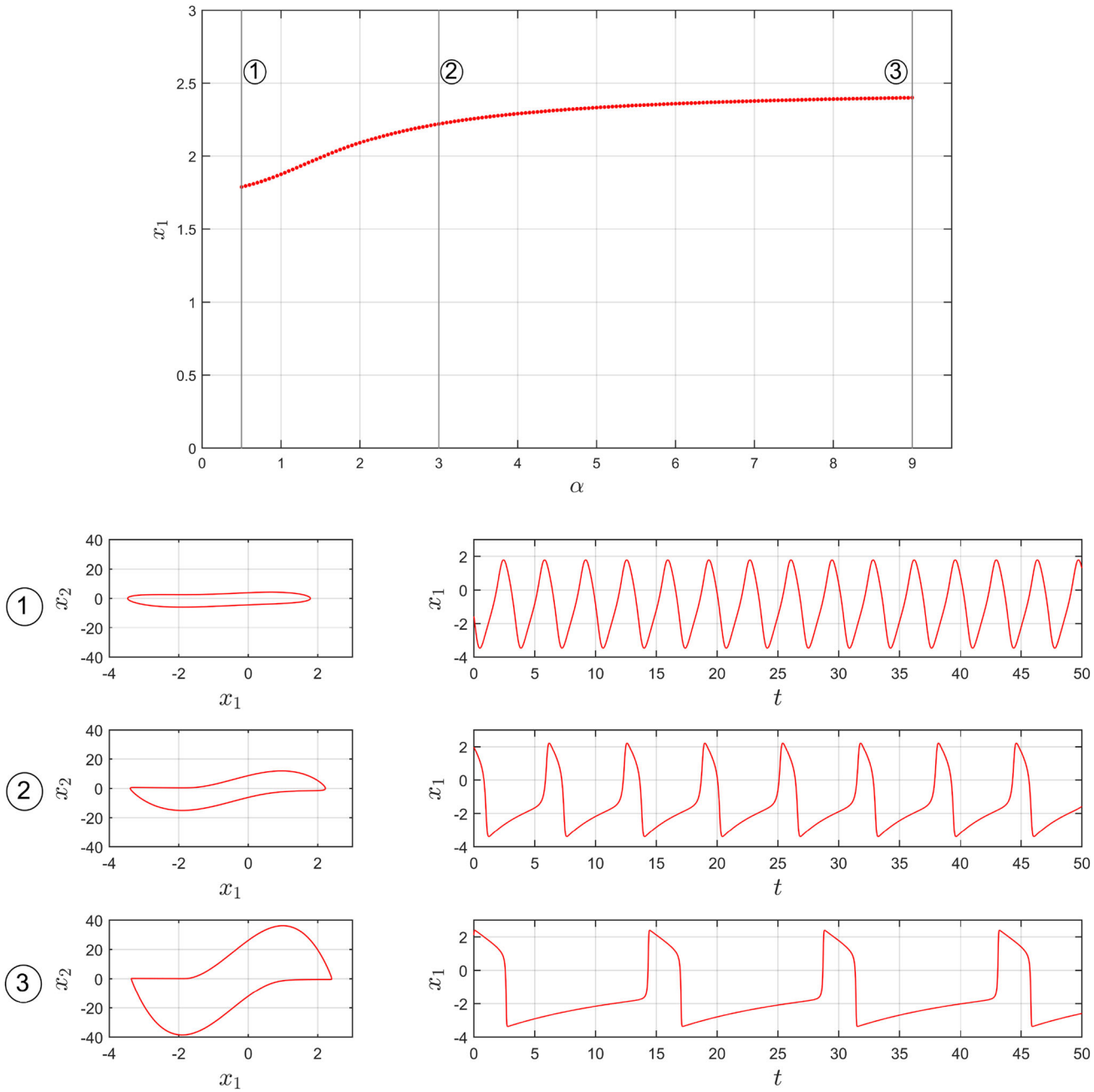

Fig. 3 Influence of dissipation α on natural pacemaker behavior. (Upper panel) Bifurcation diagram; (Bottom panel) state spaces and time series referring to numbered responses marked in diagram

9–0.19; Response 10–0.32; Response 11–0.38; Response 12–0.38; Response 13–0.38.

It should be pointed out that parameter variations result in different kinds of responses that are related to electrical activity of the heart. Natural pacemaker is the driving signal that defines the heartbeat behavior represented by the ECG. The main objective to be treated in the sequel is to establish a relation between each one of the natural pacemaker behaviors and the global electrical heart activity.

4 Cardiac system

The electrical activity of the cardiac system, represented by the ECG, is now of concern. Essentially, the ECG is governed by DDEs and numerical simulations are carried out employing the fourth order Runge–Kutta method with linear interpolation of time-delayed variables (2) [61]. Therefore, solutions for time instants before τ_{m-n} are approximated by a Taylor series expansion [10] [62].

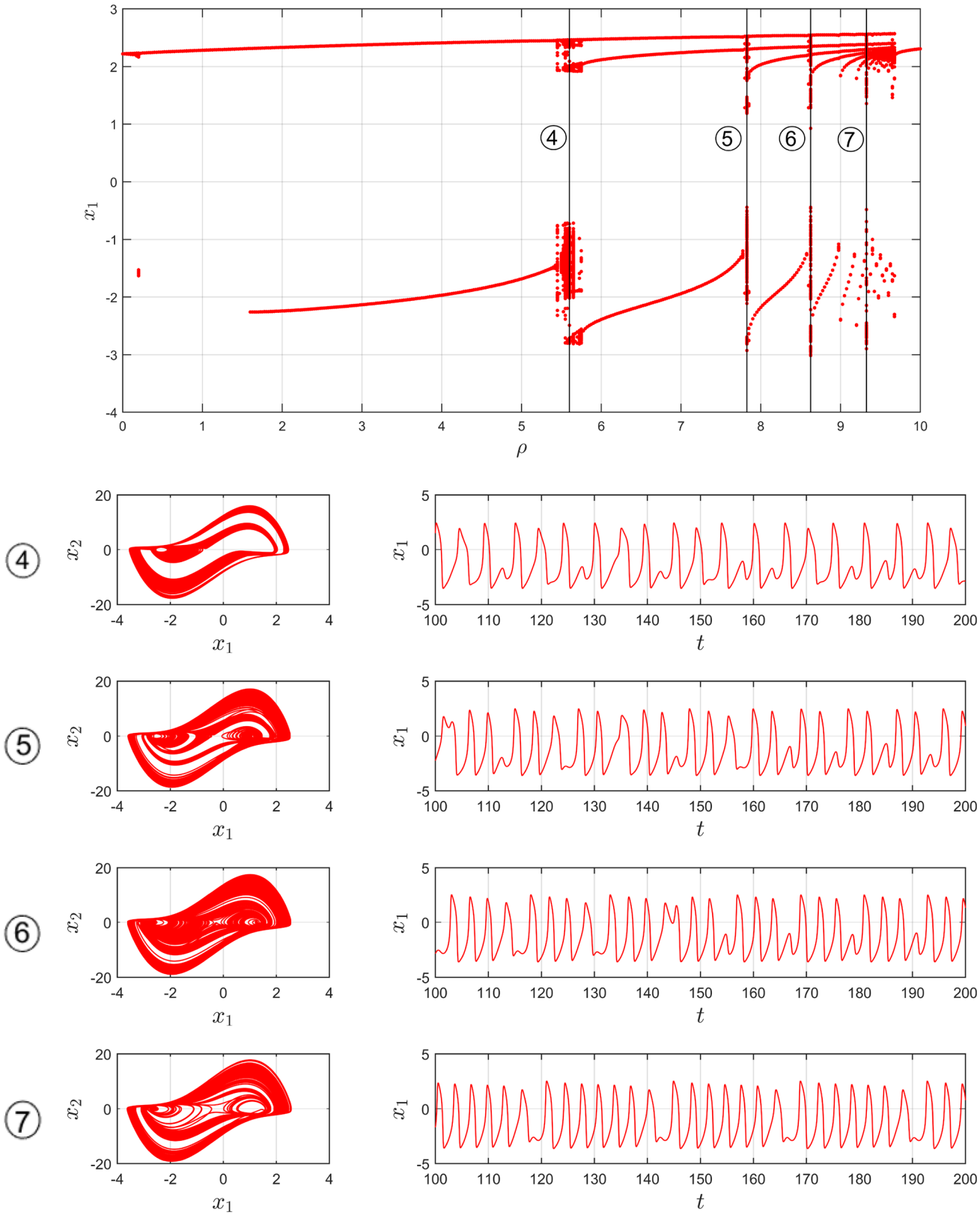

Fig. 4 Influence of external stimulus amplitude ρ on natural pacemaker behavior. (Upper panel) Bifurcation diagram; (Bottom panel) state spaces and time series reffering to numbered responses marked in diagram

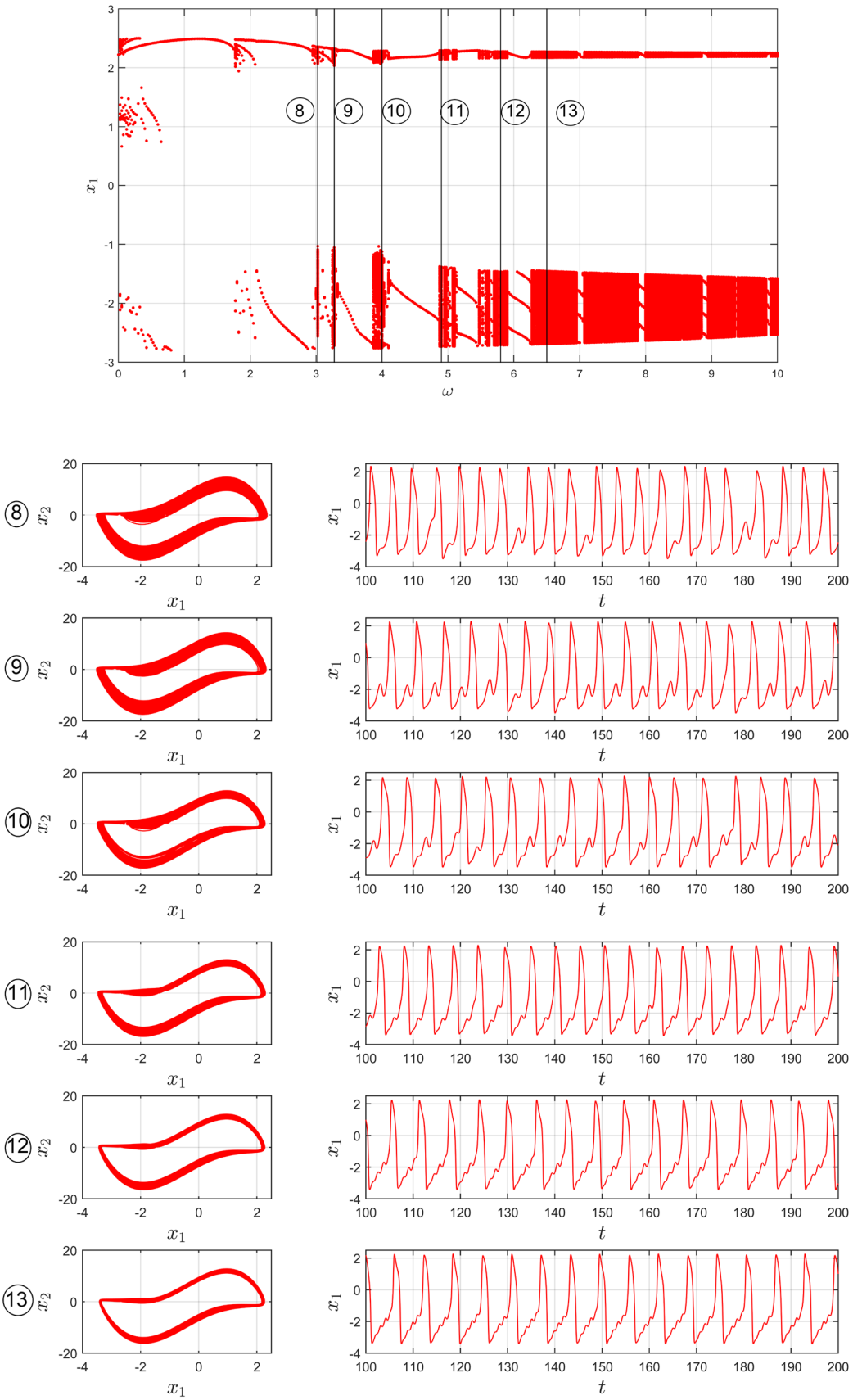

Fig. 5 Influence of external stimulus frequency ω on natural pacemaker behavior. (Upper panel) Bifurcation diagram; (Bottom panel) state spaces and time series referring to numbered responses marked in diagram

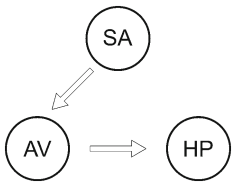

Fig. 6 Conceptual model of the normal heart functioning

Table 2 Cardiac system parameters [46]

AV node		HP complex		Couplings		Time delays	
α_{AV}	3	α_{HP}	7	k_{SA-AV}	3	τ_{SA-AV}	0.8
ν_{AV1}	0.5	ν_{HP1}	1.65	k_{AV-HP}	55	τ_{AV-HP}	0.1
ν_{AV2}	-0.5	ν_{HP2}	-2	k^{τ}_{SA-AV}	3		
d_{AV}	4	d_{HP}	7	k^{τ}_{AV-HP}	55		
e_{AV}	0.67	e_{HP}	0.67				

$$x_i^{\tau_{m-n}} = x_i - \tau_{m-n}\left(\frac{x_{i+1} - x_i}{h}\right). \tag{5}$$

A convergence analysis reveals that time steps smaller than 10^{-3} presents error of the order of 10^{-6}, considered satisfactory. In all simulations, the following parameters are used to represent the ECG as a combination of oscillator responses (units are assumed to allow a comparison with experimental real data): $\beta_0 = 1\,mV$, $\beta_1 = 0.06\,mV$, $\beta_2 = 0.1\,mV$, $\beta_3 = 0.3\,mV$. In addition, initial conditions are given by [54]:

$$\boldsymbol{x}(0) = [\ -0.1 \quad 0.025 \quad -0.6 \quad 0.1 \quad -3.3 \quad 2/3\ ]^T. \tag{6}$$

Normal heart rhythm has unidirectional couplings in such a way that the electrical impulse is conducted from SA node to AV node and then, from AV node to HP complex. As previously mentioned, external stimuli are not included in the normal rhythm. The conceptual model of this behavior is schematically represented in Fig. 6. Table 2 defines parameter values employed for the other nodes (AV and HP), vanishing all other parameters that are not presented. The SA node uses parameters presented in Table 1. All parameter are due to [46], being adjusted to match experimental data.

Figure 7 presents the dynamical rhythm associated with normal ECG. Figure 7a presents a schematic picture while Fig. 7b shows experimental data (www.physionet.org). Figure 7c shows synthetic ECG simulated with the proposed model and details of each one of the node responses, highlighting the natural pacemaker represented by the SA node. Figure 7d shows phase space related to ECG and to each one of the nodes. Note that simulations capture the main features of the experimental ECG, presenting P, QRS and T waves, being in close agreement with experimental data.

The satisfactory verification of the model to represent normal ECG encourages its use to represent other behaviors including different kinds of pathologies. In the sequence, different natural pacemaker responses are of concern, evaluating the influence of chaotic behavior on the ECGs.

4.1 Effect of the natural pacemaker behaviors

This section develops an analysis of the influence of different pacemaker behaviors on the response of cardiac system (configuration showed in Fig. 6), considering the behaviors discussed in Sect. 3. In this regard, quasi-periodic and chaotic behaviors of the natural pacemaker are employed to evaluate the resulting cardiac system behavior represented by the ECG. Each pacemaker response is associated with a number identified in the bifurcation diagrams.

Initially, situations related to the variation of the dissipation parameter α, discussed based on the bifurcation diagram of Fig. 8, are of concern. On this basis, ECG are induced by quasi-periodic responses of the natural pacemaker. Response 1 (small dissipation) exhibits higher frequency and QRS complexes with double R peaks. State space is a closed curve with 4 large loops. Response 2 presents normal rhythm showing well defined main waves and its state space is a closed curve, with two loops: a small one (around $\{0, 0\}$) and a large one (related to QRS complex). Response 3, with high dissipation, has a small frequency compared with the other cases, and double R peaks, which is a characteristic of incomplete branch blocks. The state space is formed by a closed curve with one small and two large loops.

Pacemaker responses associated with different stimulus amplitude ρ, Responses 4 to 7 selected from bifurcation diagram shown in Fig. 4, are now investigated. Figure 9 presents ECGs induced by these pacemaker signals, allowing the identification of some clinical characteristics. It is noticeable non-periodic rhythms, with irregular occurrence of R peaks, which is a characteristic of atrial tachycardia. In addition, double R peaks are identified, being associated with branch blocks. Alternations of the P and T waves are observed as well. P wave deviations are related to junctional tachycardia [63]. The development of proper methods for identification of alternation of T waves is of great interest since it is useful as clinical indicator of cardiac sudden death [64]. State spaces are characterized by filled regions around large loops, indicating a higher density of orbits than the previous cases, pointing to a more complex response that, however, it is not easy to be observed through time series.

Figure 10 presents ECGs induced by responses associated with different stimulus frequency values ω, Responses 8 to 13 selected from bifurcation diagram shown in Fig. 5. Simulated ECGs exhibit non-periodic rhythms, including alternation of single and double R peaks. It should be pointed out that these cases present deviations from normal rhythm being more pronounced in small oscillations (P and T waves). State spaces present filled regions around larger loop, with small density of orbits than the previous cases.

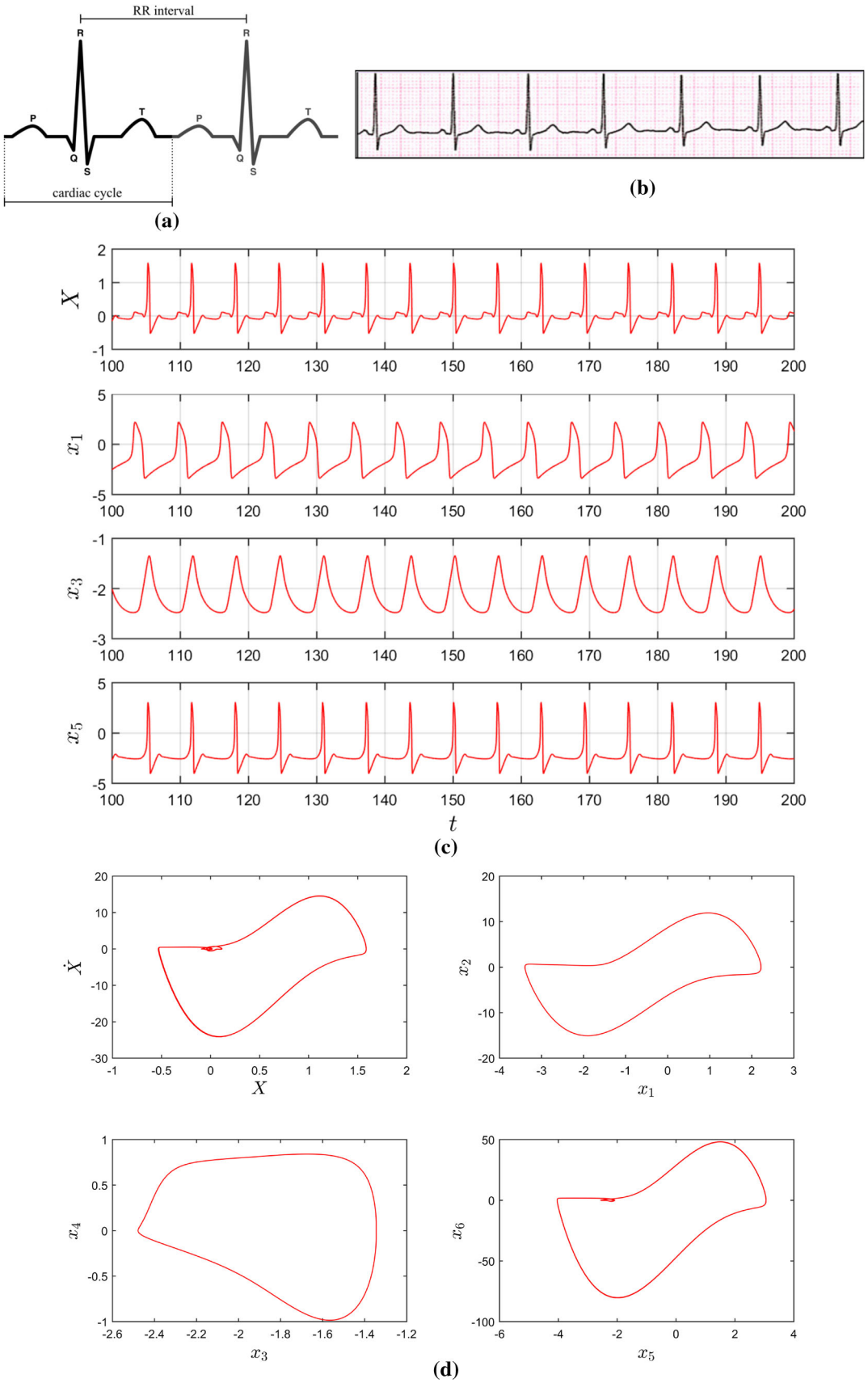

Fig. 7 Cardiac normal rhythm: **a** schematic ECG cycle; **b** experimental ECG (www.physionet.org); **c** simulated ECG and details of each one of the oscillators; **d** state spaces $\{X, \dot{X}\}$, $\{x_1, x_2\}$, $\{x_3, x_4\}$ and $\{x_5, x_6\}$

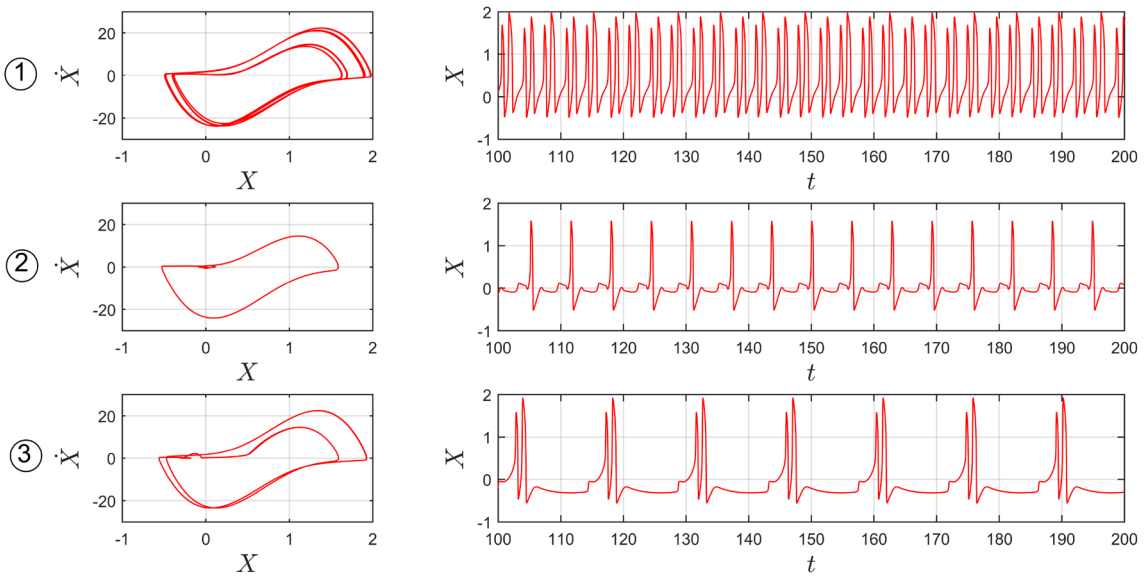

Fig. 8 Influence of dissipation α in ECGs. Each line shows simulated ECG (state space–left column, time series—right column) driven by numbered SA responses displayed in Fig. 3

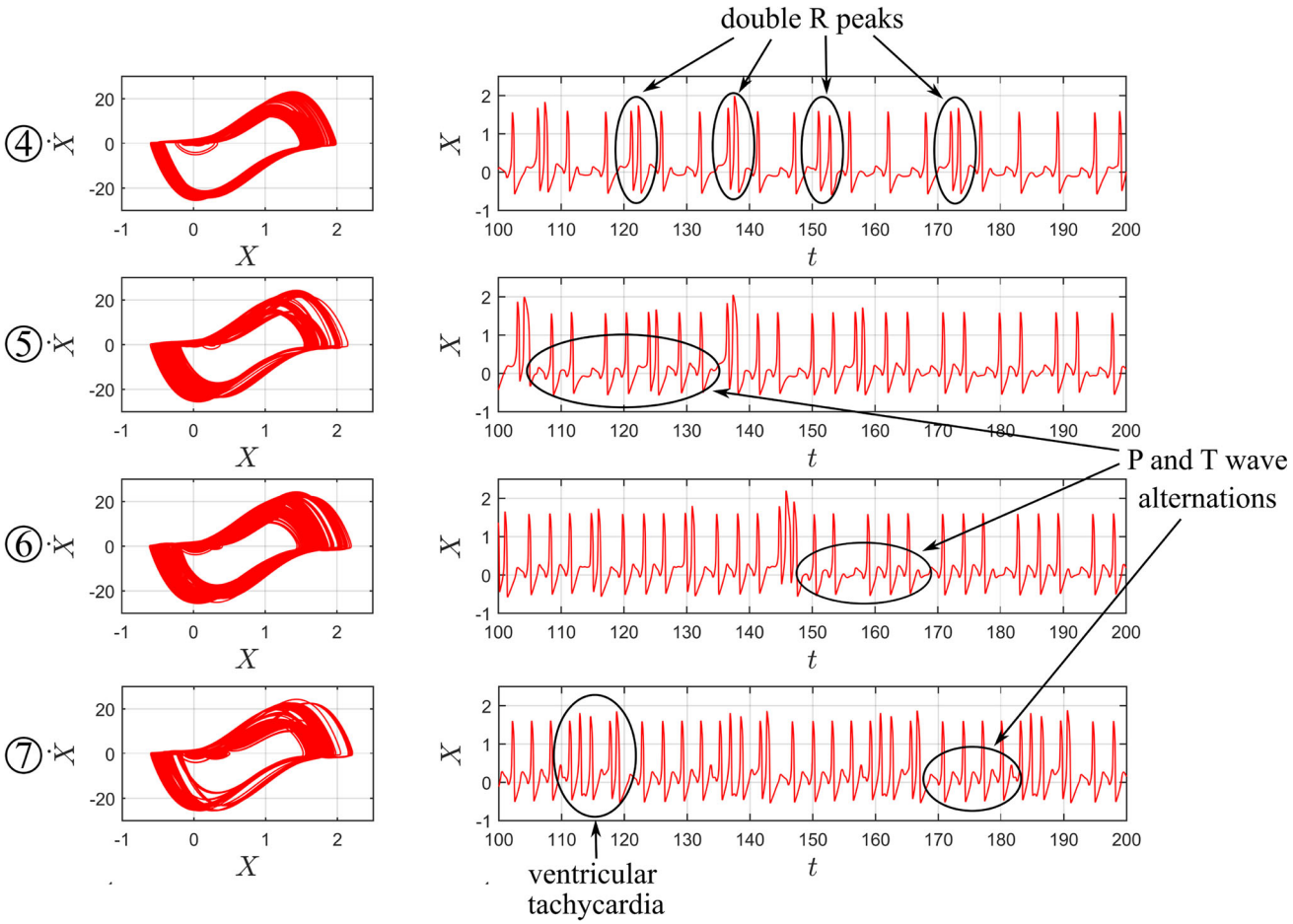

Fig. 9 Influence of stimulus amplitude ρ in ECGs. Each line shows simulated ECG (state space—left column, time series—right column) driven by numbered SA responses displayed in Fig. 4

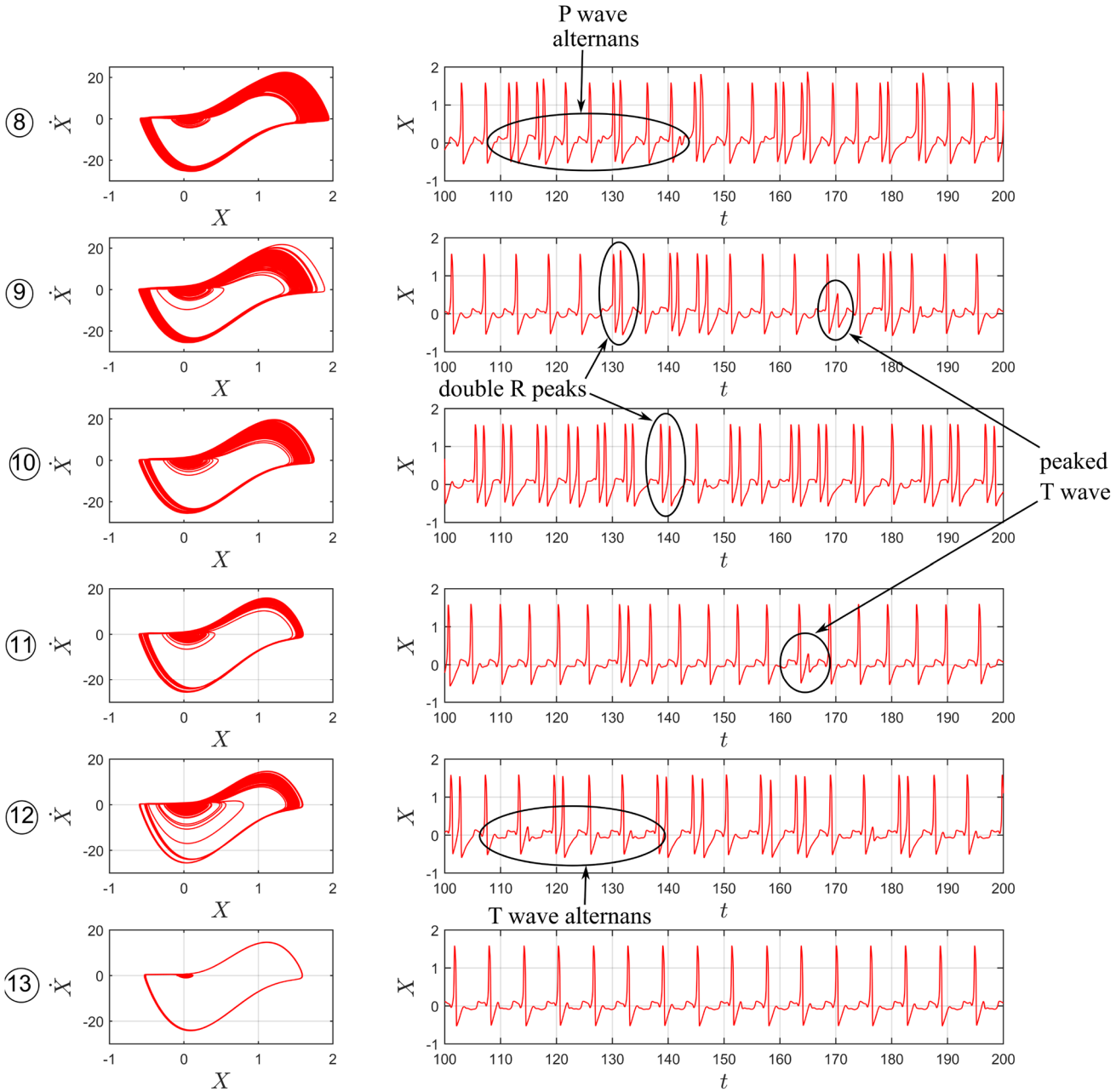

Fig. 10 Influence of stimulus frequency ω in ECGs. Each line shows simulated ECG (state space—left column, time series—right column) driven by numbered SA responses displayed in Fig. 5

5 Conclusions

This work deals with the analysis of heart nonlinear dynamics based on a mathematical model represented by the coupling of three nonlinear oscillators that represent heart nodes: sinoatrial node (SA), atrioventricular node (AV) and His–Purkinje complex (HP). Cardiovascular rhythms are investigated from different driven signals of the natural pacemaker. A global comprehension of the SA behavior is provided by an analysis of bifurcation diagrams. Distinct kinds of responses are evaluated, being classified as quasi-periodic and chaotic. The effect of these rhythms in the electrical activity of the cardiac system, represented by ECGs, is then investigated. The variety of generated ECG behaviors reveals some relevant cardiac arrhythmic responses as branch blocks and junctional tachycardia that may lead to dangerous rhythms as atrial and ventricular fibrillations. In addition, T wave alternations are identified, which is a useful information since it can be employed as clinical indicator of cardiac sudden death.

Acknowledgements The authors would like to acknowledge the support of the Brazilian Research Agencies CNPq, CAPES and FAPERJ.

References

1. M.A. Savi, J. Braz. Soc. Mech. Sci. Eng. **27**, 157–169 (2005)
2. R. Pool, Science **243**, 604–607 (1989)
3. A.L. Goldberger, D.R. Rigney, B.J. West, Sci. Am. **262**, 42–49 (1990)
4. J.E. Skinner, A.L. Goldberger, G. Mayer-Kress, R.E. Ideker, Nat. Biotechnol. **8**, 1018–1024 (1990)
5. J.N. Herbschleb, R.M. Heethaar, I. Tweel, F.L. Meijler, Comput. Cardiol. 365–368 (1980)
6. P.S. Chen, A. Garfinkel, J.N. Weiss, H.S. Karagueuzian, Chaos: Interdiscip. J. Nonlinear Sci. **8**, 127–136 (1998)
7. A.C. Skanes, R. Mandapati, O. Berenfeld, J.M. Davidenko, J. Jalife, Circulation **98**, 1236–1248 (1998)
8. L. Glass, M.C. Mackey, *From Clocks to Chaos: The Rhythms of Life* (Princeton University Press, Princeton, 1988)
9. P.E. Rapp, Biologist **40**, 89–94 (1993)
10. S.R.S.M. Gois, M.A. Savi, Chaos Sol. Fract. **41**, 2553–2565 (2009)
11. L. Glass, Chaos **19**, 028501 (2009)
12. D. Dubin, *Interpretacao Rapida Do ECG* (EPUB, Rio de Janeiro, 1996)
13. M. Malik, A.J. Camm, *Heart Rate Variability* (Futura, New York, 1995)
14. A.L. Goldberger, E. Goldberger, *Clinical Electrocardiography* (Mosby, 1977)
15. D.T. Kaplan, R.J. Cohen, Circul. Res. **67**, 886–892 (1990)
16. J. Pan, W.J. Tompkins, IEEE. Trans. Biomed. Eng. **3**, 220–236 (1985)
17. G.B. Moody, R.G. Mark, A. Zoccola, S. Mantero, Comput. Cardiol. **12**, 113–116 (1985)
18. H. Kantz, T. Schreiber, *Nonlinear Time Series Analysis, Ser. 7.* (Cambridge Nonlinear Science, USA 2002)
19. F.X. Witkowski, L.J. Leon, P.A. Penkoske, W.R. Giles, M.L. Spano, W.L. Ditto, A.T. Winfree, Nature **392**, 78–82 (1998)
20. R.K.A. Radhakrishna, D.N. Dutt, V.K. Yeragani, Auton. Neurosci. Basic Clin. **83**, 148–158 (2000)
21. P.V. Bayly, B.H. Kenknight, J.M. Rogers, E.E. Johnson, R.E. Ideker, W.M. Smith, Chaos **8**, 103–115 (1998)
22. J.Q. Zhang, A.V. Holden, O. Monfredi, M.R. Boyett, H. Zhang, Chaos **19**, 028509 (2009)
23. H.D.I. Abarbanel, R. Brown, J.B. Kadtke, Phys. Rev. A **41**, 1782–1807 (1990)
24. J.D. Farmer, J.J. Sidorowich, Phys. Rev. Lett **59**, 845–848 (1987)
25. G. Sugihara, R. May, Nature **344**, 734–741 (1990)
26. M.E.D. Gomes, A.V.P. Souza, H.N. Guimaraes, L.A. Aguirre, Chaos **10**, 398–410 (2000)
27. J.H. Lefebvre, D.A. Goodings, M.V. Kamath, E.L. Fallen, Chaos **3**, 267–276 (1993)
28. R.B. Govindan, K. Narayanan, M.S. Gopinathan, Chaos **8**, 495–502 (1998)
29. M. Barahona, C.S. Poon, Nature **381**, 215–217 (1996)
30. C.S. Poon, M. Barahona, Proc. Natl. Acad. Sci. USA **98**, 7107–7112 (2001)
31. G.Q. Wu, N.M. Arzeno, L.L. Shen, D.K. Tang, D.A. Zheng, N.Q. Zhao, D.L. Eckberg, C.S. Poon, PLoS One **4**, e423 (2009)
32. A. Wolf, J.B. Swift, H.L. Swinney, J.A. Vastano, Physica D **16**, 285–317 (1985)
33. C.K. Peng, S. Havlin, H.E. Stanley, A.L. Goldberger, Chaos **5**, 82–87 (1995)
34. J. Alvarez-Ramirez, E. Rodriguez, J.C. Echeverría, Chaos **19**, 028502 (2009)
35. M.D. Costa, C.K. Peng, A.L. Goldberger, Cardiovasc. Eng. **8**, 88–93 (2009)
36. B. van Der Pol, J. van Der Mark, Philos. Mag. **6**, 763–775 (1928)
37. G.K. Moe, W.C. Rheinboldt, J.A. Abildskov, Am. Heart J. **67**, 200–220 (1964)
38. J. Jalife, O. Berenfeld, A. Skanes, R. Mandapati, J. Cardiovasc. Electrophysiol. **9** (1998)
39. V.I. Krinsky, Pharmacol. Thera. Part B General Syst. Pharmacol. **3**, 539–555 (1978)
40. F. Fenton, A. Karma, Chaos **8**, 20–47 (1998)
41. F.H. Fenton, E.M. Cherry, H.M. Hastings, S.J. Evans, Chaos Interdiscip. J. Nonlinear Sci. **12**, 852–892 (2002)
42. J. Jalife, Ann. Rev. Physiol. **62**, 25–50 (2000)
43. M.P. Nash, A.V. Panfilov, Prog. Biophys. Mol. Biol. **85**, 501–522 (2004)
44. K. Grudzinski, J.J. Zebrowski, Physica A **336**, 153–162 (2004)
45. A.M. Dos Santos, S.R. Lopes, R.R.L. Viana, Physica A **338**, 335–355 (2004)
46. A. Cheffer, M.A. Savi, T.L. Pereira, A.S. de Paula, Appl. Math. Model. **96**, 152–176 (2021)
47. E. Ryzhii, M. Ryzhii, *International Conference on Biomedical Informatics and Technology* (Springer, Berlin, Heidelberg, 2013), pp. 67–75
48. E. Ryzhii, M. Ryzhii, Comput. Methods Prog. Biomed. **117**, 40–49 (2014)
49. G.C. Cardarilli, L. Di Nunzio, R. Fazzolari, M. Re, F. Silvestri, Appl. Sci. **9**, 3653 (2019)
50. A. Garfinkel, M.L. Spano, W.L. Ditto, J.N. Weiss, Science **257**, 1230–1235 (1992)
51. A. Garfinkel, J.N. Weiss, W.L. Ditto, M.L. Spano, Trends Cardiovasc. Med. **5**, 76–80 (1995)
52. E. Ott, C. Grebogi, J.A. Yorke, Phys. Rev. Lett. **64**, 1196–1199 (1990)
53. B.B. Ferreira, A.S. De Paula, M.A. Savi, Chaos Sol. Fract. **44**, 587–599 (2011)
54. B.B. Ferreira, M.A. Savi, A.S. De Paula, Physica Scripta **89**, 105203 (2014)
55. F. Lounis, A. Boukabou, A. Soukkou, Chaos Sol. Fract. **132**, 109581 (2020)
56. M.A. Quiroz-Juárez, O. Jiménez-Ramírez, R. Vázquez-Medina, V. Breña-Medina, J.L. Aragón, R.A. Barrio, Sci. Rep. **9**, 1–10 (2019)
57. A. Khan, U. Nigar, Int. J. Appl. Comput. Math. **6**, 1–22 (2020)
58. F.E. Yates, L.A. Benton, Math. Comput. Model. **19**, 161–170 (1994)
59. A. Cheffer, M.A. Savi, Biosystems **196**, 104177 (2020)
60. A. Cheffer, T.G. Ritto, M.A. Savi, Int. J. Non Linear Mech. **129**, 103653 (2021)
61. B. Mensour, A. Longtin, Physica D **113**, 1–25 (1998)

62. W.J. Cunningham, Proc. Natl. Acad. Sci. **40**, 708–713 (1954)
63. P. Brugada, J. Brugada, L. Mont, J. Smeets, E.W. Andries, Circulation **83**, 1649–1659 (1991)
64. P.R.B. Barbosa, J. BarbosaFilho, A.D.S. Bonfim, E.C. Barbosa, S.H.C. Boghossian, R.L. Ribeiro, P. Ginefra, Revista da SOCERJ **17**, 227–242 (2004)